A R C H I V E S O F M E T A L L U R G Y A N D M A T E R I A L S
Volume 50 2005 Issue 1

A. BORBELY* J.H. DRIVER**

DISLOCATION DENSITY MEASUREMENTS BY X-RAY PROFILE ANALYSIS IN TEXTURE COMPONENTS OF DEFORMED METALS[1)]

POMIARY GĘSTOŚCI DYSLOKACJI ZA POMOCĄ ANALIZY PROFILI LINII DLA SKŁADOWYCH TEKSTURY ODKSZTACONYCH METALI

Recent X-ray methods for determining dislocation densities in texture components of deformed metals are described. They are based on the Wilkens' model of a restrictedly random distribution of dislocations and new methods for separating out the respective broadening contributions due to strain and domain size. By appropriate choice of the goniometer angles of a diffractometer one can obtain peaks from selected texture components in a deformed metal. The basic principles for the profile analysis are described and the method then applied, using both laboratory equipment and high energy Synchrotron radiation, to the determination of the orientation dependency of stored energy in cold rolled iron and hot rolled Al-Mg. It is also shown how the results of a Taylor type crystal plasticity calculation can be used to understand anisotropic peak broadening.

Keywords: x ray diffraction, dislocation densities, rolled fcc and bcc metals, texture components.

W pracy opisano nowe metody określania gęstości dyslokacji zdeformowanego metalu odpowiadającej poszczególnym składowym tekstury. Z jednej strony bazują one na dystrybucji opartej na modelu Wilkensa a drugiej na nowej metodzie, którą zastosowano do rozseparowania wkładu wnoszonego do pszerzenia piku dyfrakcyjnego zarówno przez naprężenie jak i wielkość badanego obszaru. Poprzez właściwy wybór kątów goniometru na dyfraktometrze możliwym było uzyskanie pików odpowiadających wybranym składowym tekstury odkształconego metalu. W pracy opisano genie laboratoryjne (dyfrakcja rentgenowska) jak i wysoko energetyczne promieniowanie Synchrotronowe. Zastosowano je do określenia zależności energii zmagazynowanej do orientacji w walcowanym na zimno żelazie oraz gorąco walcowanym stopie Al.-Mg. Pokazano także jak można zastosować model

* EOTVOS LORAND UNIVERSITY, INSTITUTE FOR GENERAL PHYSICS, BUDAPEST, HUNGARY
** MICROSTRUCTURES AND PROCESSING DEPARTMENT, ECOLE DES MINES DE ST ETIENNE, CNRS FEDERATION 2145 AND UMR 5146, FRANCE

[1)] invited lecture

uplastycznienia podany przez Taylora do analizy i zrozumienia anizotropowego poszerzenia piku dyfrakcyjnego.

1. Introduction

Quantitative characterisation of the microstructures of plastically deformed metals is vital to understanding the basic mechanisms and hence the development of adequate theories of plastic deformation. Many investigations e.g. [1–3] of the deformation substructures developed in different texture components of plastically deformed iron and aluminium alloys show that a heterogeneous dislocation microstructure develops at the grain level. Different texture components have different dislocation densities with important consequences for their recrystallization behaviour. Usually, grains with higher dislocation density store higher amounts of energy and recrystallize first. The study of orientation dependent stored energy has become a major topic in many leading laboratories and new X-ray and electron microscopy methods have been developed for a more accurate description of the deformed structures. This paper reviews the work done using new X-ray line profile analyses by the co- authors during the last few years. Some of these results have been presented at the 1st Rex & GG conference [2] and others published in international journals [1, 4–5].

2. Theoretical background of advanced X-ray profile analysis

2.1. Asymptotic momentum method for the evaluation of coherent domain size and dislocation density

In the important case of plastically deformed metals of moderate to high SFE, the dislocations are arranged into cells ($T < 0.3T_f$) or sub-grain boundaries ($T > 0.4T_f$) giving rise to an additional broadening term which influences the peak widths so that the usual Fourier method of dislocation density evaluation from Bragg peaks [6] does not apply. In these conditions, the extra contribution caused by the size of the coherently scattering domain needs to be de-convoluted in order to obtain the pure strain broadening part associated with the strain field of dislocations. In the present we describe two recent methods to separate the two components. The first one is the momentum method, recently proposed by Groma [7], and based on an idea of Wilson [8]. It is appropriate for single peaks and can also be used to evaluate size anisotropy. The second method, the multiple peak or modified Williamson and Hall method, can be applied only for coherent domains with isotropic size. The momentum method takes into account the asymptotic behaviour of the second and fourth order restricted moments (RM) of the intensity distribution and has been

extended to include the size contribution [9]. No assumptions are made for the shape of the coherent domain. The k^{th} order RM is defined as follows:

$$M_k(q) = \int_{-q}^{q} q'^k I(q')dq' \Big/ \int_{-\infty}^{\infty} I(q')dq', \tag{1}$$

in which I(q) is the intensity distribution as a function of $q = 2/\lambda(\sin(\theta) - \sin(\theta_0))$, where λ is the wavelength of the X-ray, θ is the diffraction and θ_0 is the Bragg angle. Following Wilson [8] and Groma [7] for pure size and pure strain broadening, one can write the asymptotic behaviour of the second (M_2) and fourth (M_4) order RMs as below: (for practical reasons the ratio M_4/q^2 is used):

$$M_2(q) = \frac{1}{\pi^2 \varepsilon_F} q - \frac{L}{4\pi^2 K^2 \varepsilon_F^2} + \frac{\Lambda \langle \rho \rangle \ln(q/q_0)}{2\pi^2}, \tag{2}$$

$$\frac{M_4(q)}{q^2} = \frac{1}{3\pi^2 \varepsilon_F} q + \frac{\Lambda \langle \rho \rangle}{4\pi^2} + \frac{3\Lambda \langle \rho \rangle}{(2\pi)^4 q \varepsilon_F} \ln(q/q_1) + \frac{3\Lambda^2 \langle \rho^{(2)} \rangle}{4\pi^4 q^2} \ln^2(q/q_2). \tag{3}$$

The first two terms of equation (2) originate from the finite particle size, and the third one is due to dislocations. ϵ_F is the average column length, or area weighted particle size [8] measured in the direction of the diffraction vector $\boldsymbol{g}$ (it will be referred simply as domain size in the following), K is the Scherrer constant and T is the taper parameter [8] dependant on the rate of decrease of the cross section area of the crystallites. Both K and T are functions of the diffraction order hkl. In the third term $\langle \rho \rangle$ is the average dislocation density and $\Lambda = \frac{\pi}{2} g^2 b^2 C$, where g and b are the magnitudes of the diffraction and Burgers vectors, respectively. The dislocation contrast, or orientation, factor C depends on the displacement field of the dislocation and the dislocation population of different slip systems, [7]. In general C will be different for diffraction vectors pointing in different directions, even in the case of uniformly populated slip systems. A striking example of this behaviour is given in Figure 1 which plots the intensity peaks of the same texture component in rolled iron using two different diffraction vectors [1]. The peaks are quite different as a consequence of the anisotropic C coefficient. This illustrates the error involved in using the conventional Stibitz [10] formula for the stored energy W as a function of the mean relative change in lattice spacing derived from the peak width :

$$W = \frac{3}{2} E \frac{(\Delta d/d)^2}{1 + 2\nu^2}. \tag{4}$$

E is Young's modulus and ν is Poisson's ratio. The Stibitz formula predicts identical peaks for different diffraction vectors. Strictly speaking, this formula should only be applied for isotropic media which is clearly not the case of texture components. The present method, which requires an evaluation of the C coefficients, will give dislocation densities independent of the diffraction vector, as shown below.

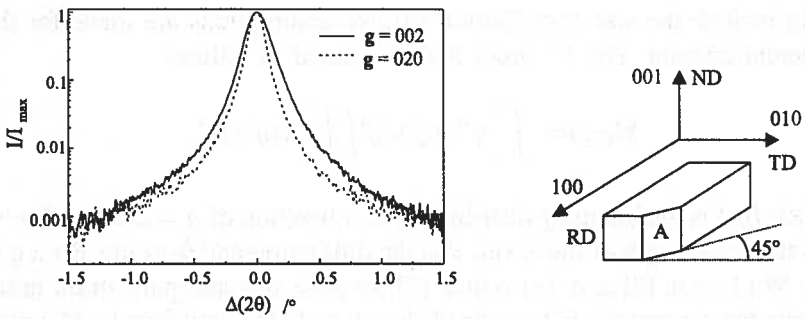

Fig. 1. 1a) Two characteristic {200} Bragg peaks measured on the {100}< 110> texture component of 88% cold rolled high purity iron. Fig. 1b) shows the sample sections

C depends on the (anisotropic) elastic displacements around dislocations [11] and also on the dislocation distributions on the slip systems. As first proposed by B o r b e l y, D r i v e r and U n g a r [1] the latter can be estimated by crystal plasticity models.

As can be seen in equation (2), the first term in M_2 related to finite size is linear in q, while dislocations give a logarithmic q dependence. The difference is more obvious in Eq. (3) for M_4, where the term due to finite domain size is again linear in q, but, at large q, the RM tends to a constant if the broadening is only due to dislocations. These characteristic behaviours are visible on the $M_k(q)$ plots so that one easily can determine by eye the characteristic type of broadening for each sample. As an example Fig. 2 shows the characteristic behaviour of the fourth order restricted moment for three different samples presenting pure size (recrystallized nano-particles of Fe), pure strain (Al-2.5%Mg deformed at room temperature) and mixed type broadening (Al-2.5%Mg deformed at 400°C).

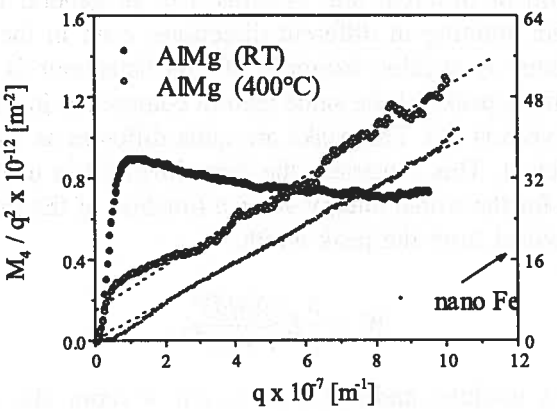

Fig. 2. Characteristic behaviour of the fourth order restricted moment of the intensity distribution for three different samples showing pure size (nanocrystalline Fe), pure strain (Al.-Mg RT) and mixed type broadening (Al.-Mg 400°C)

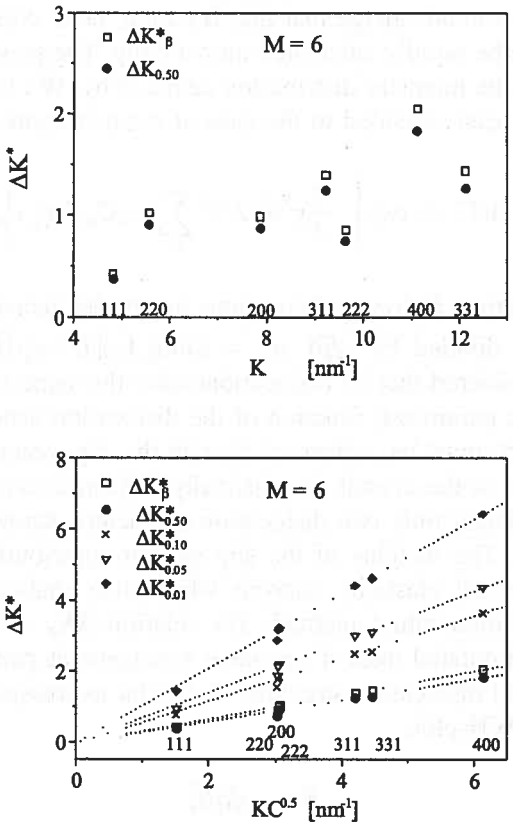

Fig. 3. a. Variation of the integral ΔK^*_β and full width at half maximum $\Delta K^*_{0.50}$ of simulated Bragg reflections for Cu with equally populated slip systems as function of K (WH plot) and Fig. 3b. Behaviour of the different ΔK^*_x widths of simulated Brag reflections for Cu with equally populated slip systems as function of $K\sqrt{C}$ (mWH plot)

2.2. Multiple peak method analysis using the Wilkens' model of a restrictedly random distribution of dislocations

According to the standard Williamson and Hall analysis of line broadening, the peak width (ΔK) is plotted as a function of the scattering vector K for a series of Bragg peaks; in theory this should give a linear plot whose slope can be used to evaluate the dislocation density. In practice the plot is not linear but exhibits discontinuities due to what is known as the strain anisotropy effect. In 1996 Borbely and Ungar [12] showed that this was related to the anisotropic contrast factor C and that the effect could be avoided by plotting $\Delta K = f(K\sqrt{C})$, known as a modified Williamson and Hall plot. Figure 3 shows this for the case of deformed pure copper. Note that this example was obtained by numerical simulations of the diffraction peaks using Wilkens' model of a restrictedly random distribution of dislocations

[13]. This model has the advantage that the Bragg peak corresponding to a given set of parameters can be rapidly calculated numerically. The general expression for the Fourier transform of the intensity distribution deduced by Wilkens for the case of one slip system, has been extended to the case of many systems "st" of weight w_{st}:

$$A(L^*) = \exp\left(-\frac{\pi}{2} g^2 b^2 (L^*)^2 \sum_{s,t} w_{st} C_{st} f(\eta^*_{st})\right), \tag{5}$$

where $C_{P}st$ is the contrast factor of dislocations having the density ρ_{st}, $L^* = L\sqrt{\rho}$, (the Fourier variable divided by $\sqrt{\rho}$), $\eta^*_{st} = |\sin(\mathbf{g}, \mathbf{l}_{st})| L^* \exp\left(\left(K_\mu\right)_{st} - 1/4\right) 2M$. For simplicity it was considered that all dislocations have the same outer cut-off radius R_e. M is a dimensionless parameter, function of the dislocation arrangement $M = R_e\sqrt{\rho}$.

The sum in eq. (5) must be performed over all the slip systems "s" and dislocation characters "t" present in the crystal. In plastically deformed crystals it is a reasonable approximation to consider only two dislocation characters, screw and edge, which are equal in number [1]. The weights of the slip system contributions are calculated by a Taylor type crystal plasticity analysis which also enables the C factors to be evaluated, as for the momentum method. The relation $\Delta K_x = \sqrt{\rho}\Delta K^*_x$ links the real peak widths to the simulated ones if the same arrangement parameter M is valid for the real and the model dislocation structure. A similar expression holds for the slopes of the lines in the mWH plot:

$$B_x = \sqrt{\rho} B^*_x, \tag{6}$$

which can be used for the evaluation of the dislocation density. Methods for evaluating the M and B parameters have been described in detail in [4].

3. Experimental results

The diffraction measurements have been carried out using both laboratory X-ray equipment and high energy Synchrotron source at the ESRF, Grenoble. Details are given in references [1, 4, 5] . Using the lab. equipment, Bragg peaks were measured on single grains belonging to different texture components, by cutting the samples parallel to the investigated hkl lattice planes and positioning them in a symmetrical diffraction geometry. For each texture component, measurements were only performed on peaks from that particular component, i.e. those which do not coincide with reflections, of similar Miller indices, from other components.

Using the high energy (18 keV) Synchrotron radiation in transmission one obtains an average information from many similarly oriented grains. The samples were irradiated by a nearly parallel X-ray beam having a cross section of $2\times0.5\text{mm}^2$ and different $\omega - 2\theta$ Laue peaks were recorded for each texture component.

3.1. Stored energy evaluation in plane-strain compressed UHP iron

Polycrystalline samples of Ultra High Purity iron about 150 μm initial grain size were deformed in plane strain compression to reductions of 48% and 62% after which cold rolling was applied to attain a final reduction of 88% [1]. Texture measurements show that in cold rolled iron two main texture fibres are developed; the γ-fibre {111} <uvw> and the α-fibre {hkl}<110>. Microhardness measurements indicate that the γ-grains are harder then the α-grains by a factor of about 1.8. Assuming a flow stress proportional to $\sqrt{\rho}$ one can conclude that the dislocation density, and consequently the related stored energy in the γ-fibre is larger, by a factor of about 3.2, than in the α-fibre. To evaluate ρ the RM method of peak profile analysis was used as given by Eqs. (2) and (3). Two fibre components were chosen, the {100}<110> α component and the {111}<112> γ component on which high-resolution Bragg peaks were measured using X-ray laboratory equipment. Fig.1a shows the 200 peaks recorded from the α component. The 002 peak was measured on the surface normal to ND, while the 020 peak was measured on the inclined surface indicated by "A" on Fig. 1b. The {111}<112> γ component was also investigated with two different diffraction vectors, the symmetric g=112 measured on the surface perpendicular to RD, and the asymmetric g=110 on the surface perpendicular to ND. The results of the evaluation for the two texture components are presented in Table 1. Note that the formal dislocation density $\rho*$ is also given here, since this parameter $\rho*$ (= $\Lambda\rho$), illustrates the influence of the dislocation contrast factor C. The differences in the formal dislocation density

TABLE

Dislocation density ρ, and stored energy W in the α_1 {100}<110> and γ_1 {111}<112> texture components at different reductions R. ϵ_F is the coherent particle size, R_{eff} is the effective outer cut-off radius of dislocations and C_{hkl} are the contrast factors. Note that the values given here are slightly different from those published initially [1] where the dislocation densities were evaluated from the initial Fourier analysis of Wilkens and not from the more recent equations (2, 3)

g	R %	ϵ_F nm	$<\rho*>$ $10^{14}m^{-2}$	C_{hkl}	$<\rho>$ $10^{14}m^{-2}$	R_{eff} nm	W J/mol
002	48	160	3.2	0.3256	2.1	34	4.4
(α_1	62	94	3.5	0.3254	2.2	31	4.4
	88	93	3.2	0.3254	2.1	54	4.1
020	48	195	2.1	0.2178	1.9	31	4.2
(α_1)	62	169	3.0	0.2176	2.9	34	6.2
	88	150	2.2	0.2176	2.1	27	4.5
112	48	104	2.8	0.1274	3.1	28	6.3
(γ_1)	62	57	6.6	0.1285	7.2	18	13.0
	88	53	6.4	0.1301	6.9	17	12.3
110	48	121	1.0	0.1433	3.0	30	6.1
(γ_1)	62	92	2.7	0.1453	7.7	20	15.2
	88	62	2.8	0.1503	7,9	22	14.5

$< \rho* >$, presented in Table 1 can only be explained by the different C_{hkl} for the diffraction vectors. This is possible when the active slip systems during deformation are non-uniformly populated. Crystal plasticity calculations for plane strain compression have been used to estimate the dislocation distributions on the {110} and {112} slip planes [1]. The simulated dislocation density on a slip system was considered to be composed of a mobile part, related to the slip rate via the Orowan formula and a statistical dislocation density taken as a fraction of the dislocations produced during a deformation step. Taking the simulated dislocation densities as weighting factors an average value of the contrast factors was then calculated (Table 1). According to this Table the coherent domain size εF decreases with deformation and takes values of the order of 100 nm. The final values of the stored energy were calculated from the standard relation

$$W = \frac{Kb^2}{4\pi}\rho \ln (R_e/r_0), \tag{7}$$

where K is the dislocation energy factor, and the outer cut-off radius R_e is taken as equal to the coherent domain size ϵ_F, giving an upper limit. The data for the stored energies are somewhat smaller than the average value of 19 J/mol obtained by calorimetry on the same material [14] but in good agreement with the results of Ref. [15] for cold rolled (70% reduction) low-carbon steel.

3.2. Stored energy evaluation in hot plane-strain compressed Al-2.5% Mg

Hot deformation of Al alloys develops sub-grain type structures by dynamic recovery which, in the case of Al-Mg, contain free dislocations; there are therefore dislocation strain field and domain size contributions which have to be de-convoluted in a system of relatively low dislocation density. This is a major challenge for the X-ray method. As part of a study of recrystallization, Al-2.5%Mg (AA5052) polycrystalline samples of about 50 μm initial grain size were deformed at 400°C in plane strain compression to logarithmic strains of 0.2 to 1.4, using a channel die set-up. High resolution X-ray Bragg peaks were measured in the laboratory on 5 different texture components i.e. Brass (110)[-112], Cube (001)[100], Goss (110)[001], Copper (112)[11-1] and S (123)[41-2]. These texture components represent about 65-70% of the total orientations present in the polycrystal (for samples deformed to 1.4 strain), which means that the chosen Bragg reflections will correspond with high probability to the selected ideal orientations. The X-ray peaks were first evaluated according to the momentum method described in section 2.1. and the average dislocation densities are shown in Figure 4.

In this initial investigation only one *hkl* reflection type was measured on each texture component and to obtain the dislocation density we have assumed an equal population of dislocations on the different slip systems. For dynamically recovered structures it turns out that this assumption is not unreasonable and the data of Fig. 4.b. reflect qualitatively well the differences in dislocation densities of the texture components. According to this figure the highest dislocation density develops in the S component, while the Brass, Cube and Goss components have the lowest values. In

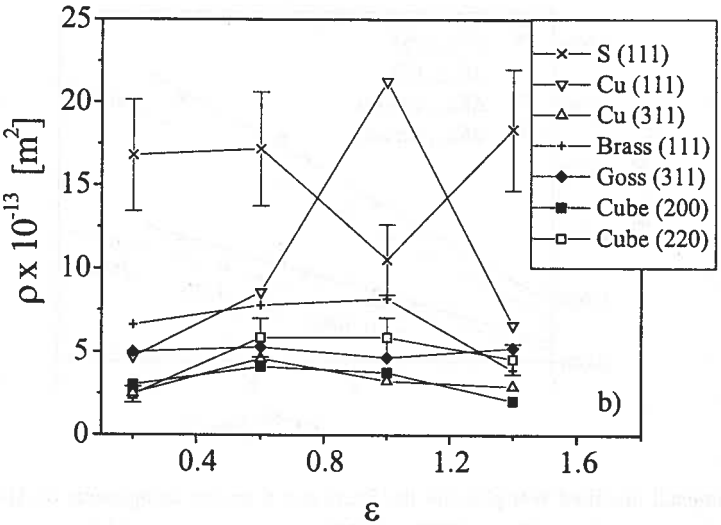

Fig. 4. Average dislocation density in the texture components of Al.-2.5% Mg measured by the momentum methods as a function of plane strain compression at 400°C and 1/s. (The numbers in brackets indicate the Bragg peaks used for the evaluation)

general the average domain size decreases with deformation in all texture components with values between 100nm and 700nm at the highest deformation (ϵ = 1.4). After a relatively monotonic decrease to strains of about ϵ = 0.6, the domain size tends to stabilise although some components, particularly the cube, appear to have a rather erratic behaviour.

To improve the analysis of the dislocation microstructure in the hot-deformed Al-Mg alloy, experimental investigations were done on the high-resolution powder diffraction beamline BM16 at ESRF. Due to the high X-ray flux and better experimental facilities, 5 different *hkl* peaks could be measured on each texture component of the deformed samples. This facilitated studying the strain anisotropy of the samples from which important information on the distribution of the dislocations on different slip systems could be obtained. However, we often found an extra broadening contribution to the tails of the X-ray peaks, and the momentum method could not be used for all the peaks. In fact. the central region part of the peaks down to a relative intensity value of about 5% is not influenced by this extra broadening and can be used in the *m*WH plot. The application of the mWH plot requires, however, a knowledge of the distribution of the dislocations on the different slip systems from which the average contrast factor for a given diffraction vector should be calculated. Again using the idea proposed in [1], the dislocation population of the different slip systems were estimated from crystal plasticity calculations. For the Al-2.5Mg alloy deformed at 400°C, plastic slip on the octahedral and non-octahedral slip systems was assumed and a relaxed constraints Taylor-model used to simulate the texture evolution [16]. It was assumed that the dislocation density on a slip system is proportional to the amount of slip

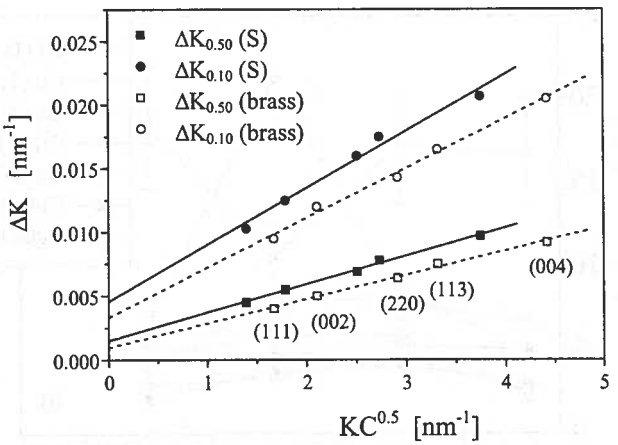

Fig. 5. Experimental modified WH plots for the Brass and S texture components of Al-2.5% Mg alloy deformed in hot PSC at 400°C $1sec^{-1}$ to a strain of 1.4

on that system and, due to isotropic hardening, half of the dislocations produced in one deformation step will appear equally distributed on the non-activated slip systems. Given these estimated dislocation density populations, the average contrast factors were calculated and used as weighting factors in the mWH plot. The plots corresponding to different peak-widths are presented in Figure 5 for the case of the Brass and S texture components. It is seen that these texture components can be well fitted by a straight line (also true for the Goss component). The fit worsens for the Copper component (15% error) and has a very large error of about 40% for the cube component, Figure 6.

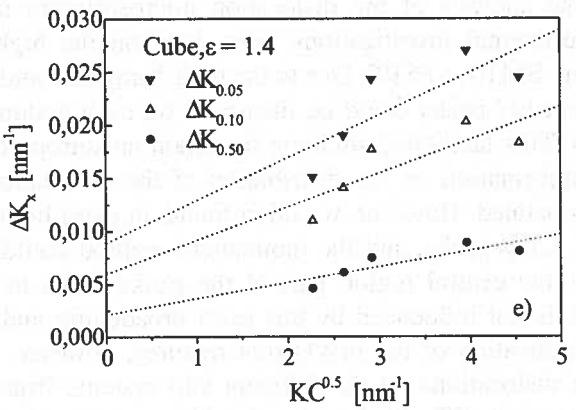

Fig. 6. Experimental modified WH plots for the cube texture component of Al.-2.5% Mg alloy deformed in hot PSC at 400°C $1sec^{-1}$ to a strain of 1.4

The dislocation density was evaluated for each texture component from the *m*WH plots by comparing the measured and simulated peaks for each component. The results

shown in Fig. 7 have the same qualitative behaviour as those obtained in the laboratory. The *S* component has the highest dislocation density, and is larger by a factor of about 2 than the dislocation density of the other components. The absolute values of ρ are in agreement with previous data for most of the components, excepting *S*, which is somewhat smaller in this case. The error bar in Figure 7 is 20%.

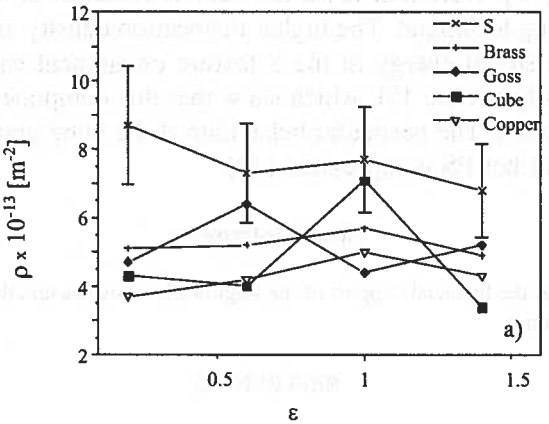

Fig. 7. Average dislocation density in texture components of Al.-2.5%MG measured by the modified WH methods as a function of plane strain compression at 400°C and 1/s

The arrangement parameter *M*, introduced by W i l k e n s was also evaluated as 2.6 for the Brass, Goss, Copper and Cube components and 2.7 for the S component. The almost identical values of *M* indicate a that the dislocation arrangement is similar in all the components. The outer cut-off radius evaluated form the equation $M = R_e \sqrt{\rho}$, yields a value of about 300-350 nm. This cut-off radius is nearly equal for all texture components so that the stored energy is mainly affected by the dislocation density.

4. Discussion and conclusions

Two X-ray methods have been developed to evaluate dislocation densities in plastically deformed crystals. The momentum method is well suited for crystals where, beside dislocations, the broadening of the peaks is influenced by the small size of the coherent domain. This method was applied for the evaluation of the dislocation density from Bragg peaks, measured in the home lab on both cold rolled iron and hot deformed Al-Mg. In the case of cold rolled iron the stored energies vary from 4.5 to 15 J/mole.

The *modified* WH plot of the peak-widths corresponding to different relative intensity ratios can be applied if the asymptotic regions, i.e. the tails of the peaks, are unavailable. This method was developed to facilitate the evaluation of the X-ray peaks measured on the hot deformed Al-Mg at ESRF, when an extra broadening term of unknown origin perturbed the tails of the peaks. Allowing for the use of different

experimental conditions for different methods, the agreement between the two sets of results obtained on the hot deformed Al-Mg alloy can be considered as being good. Nearly the same value of the dislocation density was obtained with both methods in 4 of the 5 main texture components. The corresponding stored energy of about 1 J/mol (2 J/mol for the S component) is in good correlation with stored energy data obtained by TEM [17]. Note that these are very low values of stored energy for the X-ray line broadening technique. The higher dislocation density and the corresponding higher value of the stored energy in the S texture component can be correlated with the recrystallization behaviour [5], which show that this component is often consumed first by recrystallization. The particular behaviour of the cube grains is consistent with their metastability in hot PS compression [18].

Acknowledgements

A. B. acknowledges the financial support of the Region Rhône-Alpes and the Hungarian OTKA (No. T-34999) and Bolyai Grants.

REFERENCES

[1] A. Borbély, J.H. Driver, T. Ungár, Acta mater. **48**, 2005-2016 (2000).
[2] A. Borbély, J.H. Driver in, G. Gottstein, D.A. Molodov (eds.) Recrystallization and Grain Growth, Proc. of the 1st Joint Int. Conf., 635, Springer-Verlag (2001).
[3] J-Ch. Glez, J.H. Driver, Acta Mater. **51**, 2989-3003 (2003).
[4] A. Borbély, G. Guiglionda, J.H. Driver, Z. für Metallkunde **93**, 689-693 (2002).
[5] G. Guiglionda, A. Borbely, J.H. Driver, Acta Mater. **52**, 3413- 3423 (2004).
[6] I. Groma, T. Ungár, M. Wilkens, J. Appl. Crystallogr. **21**, 47 (1988).
[7] I. Groma, Phys. Rev. **B57**, 7535 (1998).
[8] A.J.C. Wilson, Proc. Phys. Soc. **80**, 286 (1962).
[9] A. Borbély, I. Groma, Appl. Phys. Lett. **79**, 1772 (2001).
[10] G.R. Stibitz, Phys. Rev., 49, 872 (1937).
[11] A. Borbély, J. Dragomir, G. Ribarik, T. Ungár, J. Appl. Cryst. **36** 160-2 (2003).
[12] T. Ungár, A. Borbély, Appl. Phys. Lett. **69**, 3173 (1996).
[13] M. Wilkens, Fundamental Aspects of Dislocation Theory, Vol. II, edited by J A. Simmons, R. de Wit and R. Bullough, pp. 1195-1221. Natl Bur. Stand. (US) Spec. Publ. No. 317, Washington, DC (1970).
[14] F. Scholz, J.H. Driver, E. Woldt, Scripta Mater, 40, 949-954 (1999).
[15] R.L. Every, M. Hatherly, Texture, **1**, 183-194 (1974).
[16] C. Maurice, J.H. Driver, Acta Mater. **45**, 4639 (1997).
[17] T. Pettersen, A. Bardal, I. Lindseth, E. Nes, Proc. "ReX'96:. Recrystallization and Related Phenomena", eds. T.R. McNelley, Monterey, CA, USA, 495-501.
[18] C. Maurice, J.H. Driver, Acta Metall. Mater **41**, 1644 (1993).

Received: 24 January 2005.